Supporting Information

Tin dioxide buffer layer assisted efficiency and stability of wide bandgap inverted perovskite solar cells

Bingbing Chen [1, 2, 3, 4, #], Pengyang Wang [1, 2, 3, 4, #], Ningyu Ren [1, 2, 3, 4, 5], Renjie Li [1, 2, 3, 4], Ying Zhao [1, 2, 3, 4], Xiaodan Zhang [1, 2, 3, 4, †]

[1] Institute of Photoelectronic Thin Film Devices and Technology, Renewable Energy Conversion and Storage Center, Solar Energy Conversion Center, Nankai University, Tianjin 300350, China

[2] Key Laboratory of Photoelectronic Thin Film Devices and Technology of Tianjin, Tianjin 300350, China

[3] Engineering Research Center of Thin Film Photoelectronic Technology of Ministry of Education, Tianjin 300350, China

[4] Collaborative Innovation Center of Chemical Science and Engineering (Tianjin), Tianjin 300072, P.R. China

[5] School of Physical Science and Technology, Inner Mongolia University, Key Laboratory of Semiconductor, Hohhot 010021, China

Bingbing Chen and Pengyang Wang contributed equally to this work.

Correspondence to: X D Zhang, xdzhang@nankai.edu.cn

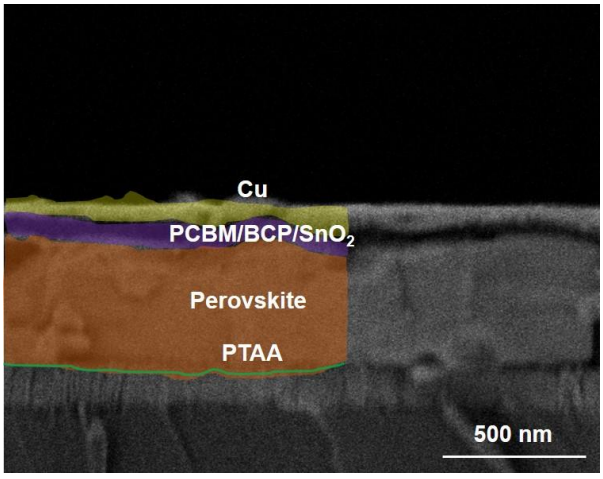

Fig. S1. The cross-sectional SEM image of perovskite solar cell with the structure of ITO/PTAA/Perovskite/PCBM/BCP/SnO_2/Cu, the scale bar is 500 nm.

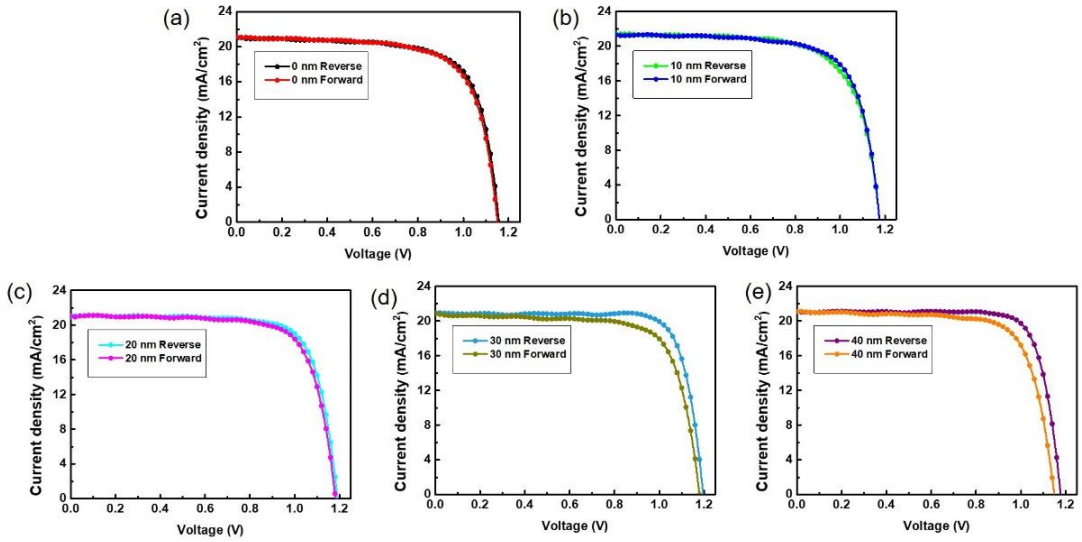

Fig. S2. *J–V* curves of IPSCs based on different thickness of SnO_2.

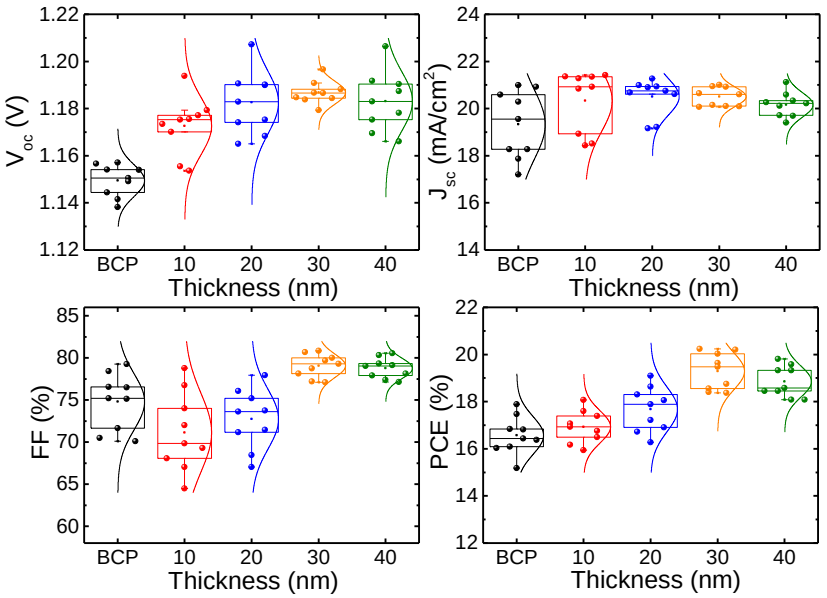

Fig. S3. Statistical *J–V* parameters of the devices with different thickness of SnO_2 films.

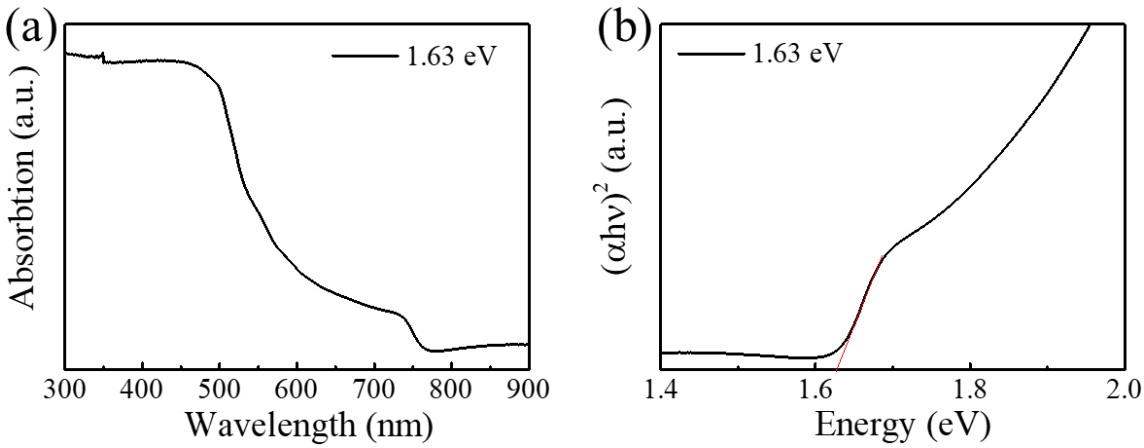

Fig. S4. (a) Ultraviolet-visible absorption of perovskite material. (b) $(\alpha h\nu)^2$ versus energy of perovskite film. The band gap of perovskite can be determined by tangent of the curve to the base line. It can be found that the band gap of the perovskite is about 1.63 eV.

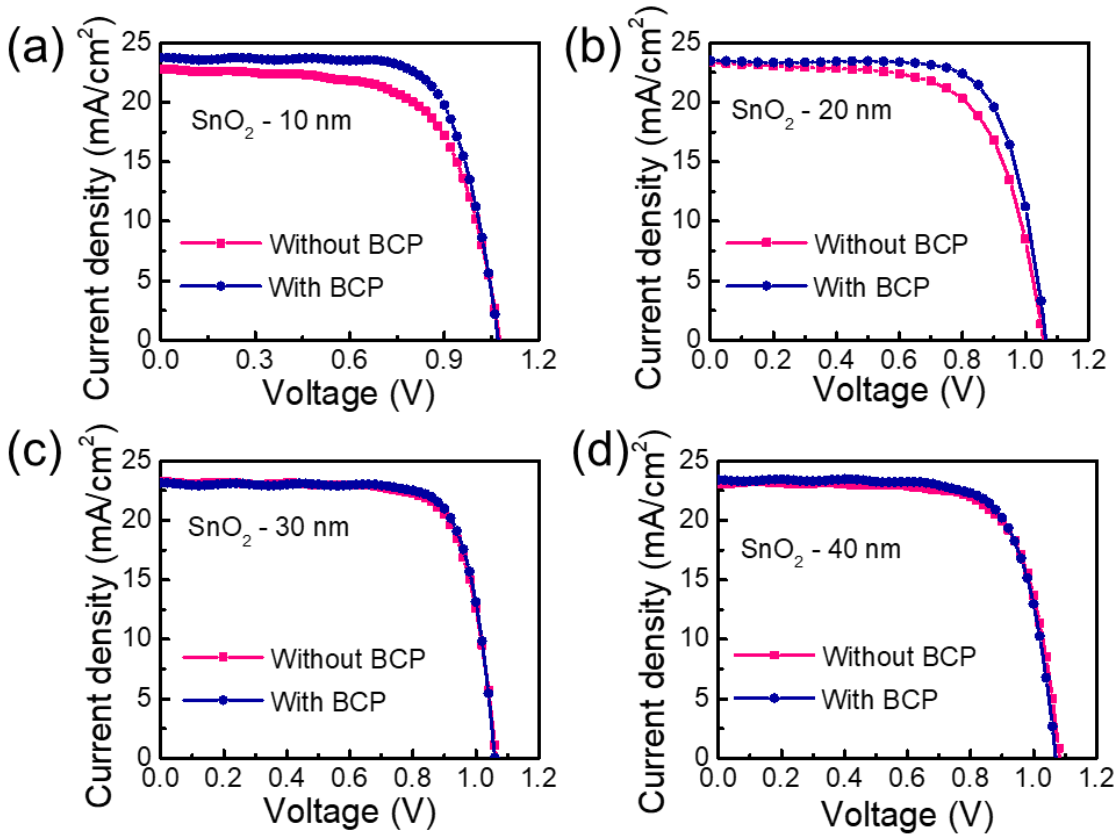

Fig. S5. *J–V* curves of the devices of different SnO_2 thickness with or without BCP.

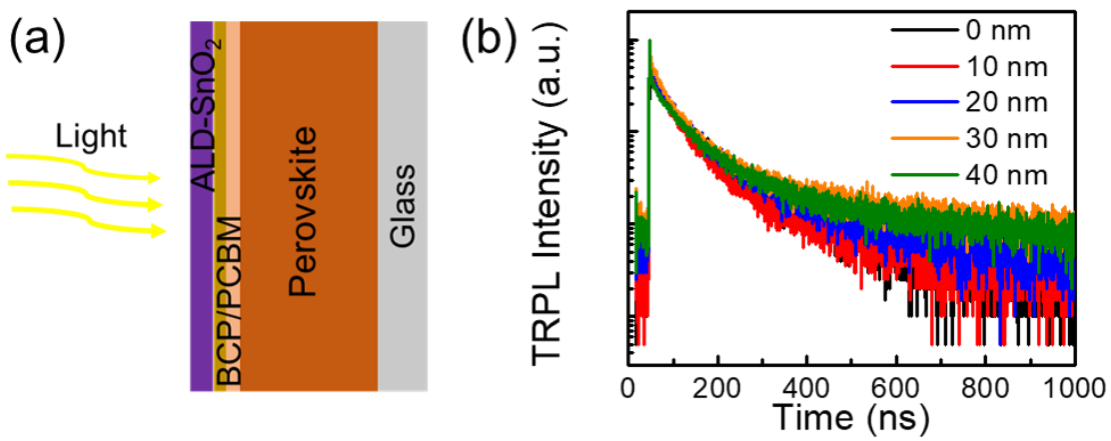

Fig. S6. (a) The structure of the sample with different SnO_2 thickness for TRPL measurement. (b) TRPL curves with different SnO_2 thickness.

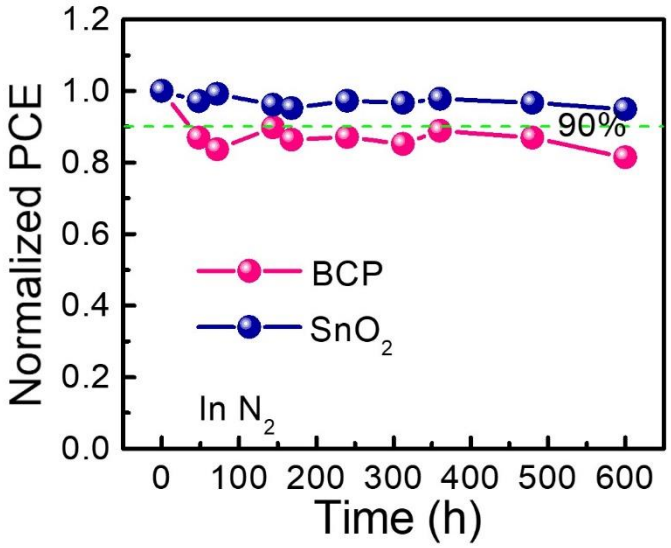

Fig. S7. Normalized PCE of perovskite devices without and with 30 nm SnO_2 kept in glove box with N_2 for 600 hours.

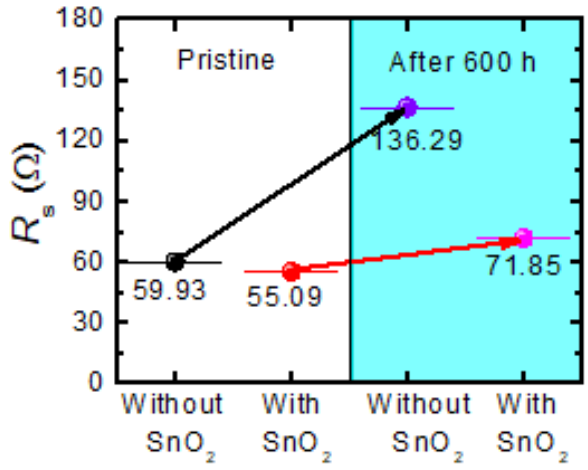

Fig. S8. The changes of R_s for the devices without and with SnO_2 in atmosphere (25 °C, 20–40 RH%) without encapsulation.

Table S1 Device performance parameters with deferent thickness of SnO_2 buffer layer. The scanning direction from 1.2 to 0 V denote as forward scan and from 0 to 1.2 V as reverse scan.

Thickness (nm)	Scanning direction	V_{OC} (V)	J_{SC} (mA/cm$_2$)	FF (%)	PCE (%)
0	Forward	1.157	20.99	71.65	17.47
	Reverse	1.151	21.13	70.51	17.21
10	Forward	1.176	21.35	69.83	17.60
	Reverse	1.175	21.28	72.00	18.08
20	Forward	1.191	21.00	76.06	19.09
	Reverse	1.182	21.04	74.37	18.49
30 n	Forward	1.197	20.92	79.66	20.02
	Reverse	1.180	20.87	73.25	18.11
40	Forward	1.175	21.12	79.32	19.82
	Reverse	1.149	21.11	73.66	17.94

Table S2 Wide bandgap IPSCs performance statistics ($E_g \geq 1.62$ eV).

Perovskite	E_g (eV)	PCE (%)	V_{OC} (V)	E_g/e-V_{OC} (mV)	J_{SC} (mA/cm^2)	FF (%)	Years	Ref.
$MAPbI_{2.4}Br_{0.6}$	1.72	13.10	1.02	700	17.50	73.7	2015	1
$MAPbI_{2.5}Br_{0.5}$	1.72	16.60	1.16	560	18.30	78.2	2016	2
$MAPbI_{2.2}Br_{0.8}$	1.75	14.90	1.21	540	15.80	77.9	2016	2
$MAPb_{0.75}Sn_{0.25}(I_{0.4}Br_{0.6})_3$	1.73	12.59	1.04	690	15.52	78.0	2016	3
$(FA_{0.83}MA_{0.17})_{0.95}Cs_{0.05}Pb(I_{0.6}Br_{0.4})_3$	1.71	18.50	1.21	500	19.70	77.5	2017	4
$FA_{0.83}MA_{0.17}Pb(I_{0.6}Br_{0.4})_3$	1.72	17.20	1.15	570	19.40	77.0	2017	5
$FA_{0.6}Cs_{0.4}Pb(I_{0.7}Br_{0.3})_3$	1.75	16.30	1.17	580	17.50	80.0	2018	6
$MAPb(I_{1-x}Br_x)_3$	1.71	16.74	1.24	470	17.45	77.0	2018	7
$(FA_{0.95}PbI_{2.95})_{0.85}(MAPbBr_3)_{0.15}$	1.62	21.51	1.21	410	22.50	79.0	2018	8
$FA_{0.75}Cs_{0.25}Pb(I_{0.8}Br_{0.2})_3$	1.68	17.50	1.10	580	19.30	82.0	2018	9
$FA_{0.8}Cs_{0.2}Pb(I_{0.7}Br_{0.3})_3$	1.75	18.19	1.24	510	17.92	81.9	2019	10
$(FA_{0.6}Cs_{0.3}DMA_{0.1}PbI_{2.4}Br_{0.6}$	1.70	19.40	1.20	500	19.60	82.0	2019	11
$MA_{0.9}Cs_{0.1}Pb(I_{0.6}Br_{0.4})_3$	1.80	15.10	1.14	660	16.90	78.0	2019	12
$(FA_{0.65}MA_{0.20}Cs_{0.15})Pb(I_{0.8}Br_{0.2})_3$	1.68	19.50	1.17	510	21.20	79.8	2019	13
$Cs_{0.15}(FA_{0.83}MA_{0.17})_{0.85}Pb(I_{85}Br_{15})_3$	1.62	19.40	1.13	490	22.10	77.8	2019	14
$Cs_{0.15}(FA_{0.83}MA_{0.17})_{0.85}Pb(I_{80}Br_{20})_3$	1.64	19.30	1.15	490	20.90	80.4	2019	14
$Cs_{0.15}(FA_{0.83}MA_{0.17})_{0.85}Pb(I_{75}Br_{25})_3$	1.68	18.50	1.18	500	19.60	80.0	2019	14
$Cs_{0.05}(FA_{0.83}MA_{0.17})_{0.95}Pb(I_{0.8}Br_{0.2})_3$	1.63	18.40	1.10	530	21.60	78.0	2019	15
$Cs_{0.25}FA_{0.75}Pb(Br_{0.2}I_{0.8})_3$	1.67	19.66	1.14	530	20.34	85.0	2020	16
$FA_{0.75}Cs_{0.25}Pb(I_{0.8}Br_{0.2})_3$	1.68	20.42	1.217	463	20.18	83.6	2020	17
$(FA_{0.64}MA_{0.20}Cs_{0.15})Pb_{0.99}(I_{0.79}Br_{0.2})_3$	1.68	21.00	1.196	484	21.65	81.5	2020	18
$Cs_{0.05}(FA_{0.77}MA_{0.23})_{0.95}Pb(I_{0.77}Br_{0.23})_3$	1.68	20.80	1.224	456	20.70	82.0	2020	19
$FAMAPb_2(I_xBr_{1-x})_3$	**1.63**	**21.13**	**1.19**	**440**	**21.86**	**81.1**	**2021**	**This work**

Table S3 The carrier extraction time and lifetime of perovskite films deposited with diffident thickness of SnO_2 buffer layer.

Thickness (nm)	0	10	20	30	40
τ_1	42.01	34.56	39.12	37.65	49.71
τ_2	146.43	136.76	154.96	181.57	198.78

References

[1] Bi C, Yuan Y, Fang Y, *et al.* Low-temperature fabrication of efficient wide-bandgap organolead trihalide perovskite solar cells. Adv Energy Mater, 2015, 5, 1

[2] Hu M, Bi C, Yuan Y, *et al*. Stabilized wide bandgap $MAPbBr_xI_{3-x}$ perovskite by enhanced grain size and improved crystallinity. Adv Sci, 2016, 3, 1

[3] Yang Z, Rajagopal A, Jo S B, *et al*. Stabilized wide bandgap perovskite solar cells by tin substitution. Nano Lett, 2016, 16, 7739

[4] Lin Y, Chen B, Zhao F, et al. Matching charge extraction contact for wide-bandgap perovskite solar cells. Adv Mater, 2017, 29, 1

[5] Zheng X, Chen B, Dai J, *et al*. Defect passivation in hybrid perovskite solar cells using quaternary ammonium halide anions and cations. Nat Energy, 2017, 2, 1

[6] Bush K A, Frohna K, Prasanna R, *et al*. Compositional engineering for efficient wide band gap perovskites with improved stability to photoinduced phase segregation. ACS Energy Lett, 2018, 3, 428

[7] Khadka D B, Shirai Y, Yanagida M, *et al*. Tailoring the open circuit voltage deficit of wide bandgap perovskite solar cells using alkyl chain substituted fullerene derivatives. ACS Appl Mater Interfaces, 2018, 10, 22074

[8] Luo D, Yang W, Wang Z, *et al*. Enhanced photovoltage for inverted planar heterojunction perovskite solar cells. Science, 2018, 360, 1442

[9] Bush K A, Manzoor S, Frohna K, *et al*. Minimizing current and voltage losses to reach 25% efficient monolithic two-terminal perovskite−silicon tandem solar cells. ACS Energy Lett, 2018, 3, 2173

[10] Chen C, Song Z, Xiao C, *et al*. Achieving a high open-circuit voltage in inverted wide-bandgap perovskite solar cells with a graded perovskite homojunction. Nano Energy, 2019, 61, 141

[11] Palmstrom A F, Eperon G E, Leijtens T, *et al*. Enabling flexible all-perovskite tandem solar cells. Joule, 2019, 3, 1

[12] Xie Y M, Ma C, Xu X, *et al*. Revealing the crystallization process and realizing uniform 1.8 eV MA-based wide-bandgap mixed-halide perovskites via solution

engineering. Nano Research, 2019, 12, 1033

[13] Kim D H, Muzzillo C P, Tong J, *et al*. Bimolecular additives improve wide-band gap perovskites for efficient tandem solar cells with CIGS. Joule, 2019, 3, 1

[14] Chen B, Yu Z, Liu K, *et al*. Grain engineering for perovskite/silicon monolithic tandem solar cells with efficiency of 25.4%. Joule, 2019, 3, 1

[15] Mazzarella L, Lin Y H, Kirner S, *et al*. Infrared light management using a nanocrystalline silicon oxide interlayer in monolithic perovskite/silicon heterojunction tandem solar cells with efficiency above 25%. Adv Energy Mater, 2019, 9, 1803241

[16] Boyd C C, Shallcross R C, Moot T, *et al*. Overcoming redox reactions at perovskite nickel oxide interfaces to boost voltages in perovskite solar cells. Joule, 2020, 4, 1

[17] Xu J, Boyd C C, Yu Z J, *et al*. Triple-halide wide–band gap perovskites with suppressed phase segregation for efficient tandems. Science, 2020, 367, 1097

[18] Kim D, Jung H J, Park I J, *et al*. Efficient, stable silicon tandem cells enabled by anion-engineered wide-bandgap perovskites. Science, 2020, 368, 1

[19] Al-Ashouri A, Köhnen E, Li B, et al. Monolithic perovskite/silicon tandem solar cell with >29% efficiency by enhanced hole extraction. Science, 2020, 370, 1